

Cosmic Reionization Redux

Nickolay Y. Gnedin^{1,2} and Xiaohui Fan³

ABSTRACT

We show that numerical simulations of reionization that resolve the Lyman Limit systems (and, thus, correctly count absorptions of ionizing photons) have converged to about 10% level for $5 < z < 6.2$ and are in reasonable agreement (within 10%) with the SDSS data in this redshift interval. The SDSS data thus constraint the redshift of overlap of cosmic HII regions to $z_{\text{OVL}} = 6.1 \pm 0.15$. At higher redshifts, the simulations are far from convergence on the mean Gunn-Peterson optical depth, but achieve good convergence for the mean neutral hydrogen fraction. The simulations that fit the SDSS data, however, do not have nearly enough resolution to resolve the earliest episodes of star formation, and are very far from converging on the precise value of the optical depth to Thompson scattering - any value between 6 and 10% is possible, depending on the convergence rate of the simulations and the fractional contribution of PopIII stars. This is generally consistent with the third-year *WMAP* results, but much higher resolution simulation are required to come up with the sufficiently precise value for the Thompson optical depth that can be statistically compared with the *WMAP* data.

Subject headings: cosmology: theory - cosmology: large-scale structure of universe - galaxies: formation - galaxies: intergalactic medium

1. Introduction

Bad things comes in threes - but good things sometimes do too. At least, in twos. In the reionization research, the two are the latest analysis of the Lyman- α absorption in the spectra of 19 highest redshift SDSS quasars by Fan et al. (2006) and the large downward revision of the *WMAP*-measured value for the Gunn-Peterson optical depth (Page 2006; Spergel 2006).

The latest SDSS data are consistent with the end of reionization epoch at $z \sim 6$ (Fan et al. 2006). The downward revision of the *WMAP* measurement now eliminates any need for complex scenarios of early reionization (c.f. Melchiorri et al. 2005, and references therein), which had to invoke unknown or weakly constrained physics and which were at odds with the simplest reionization

scenario in which normal PopII stars are the dominant source of ionizing photons between $z \sim 20$ and $z \sim 5$.

In this simplest scenario (Gnedin 2000, 2004; Roy Choudhury & Ferrara 2006) - which we call the “Minimal Reionization Model” - PopIII stars and other exotic objects play an important but not a dominant role in reionizing the universe by $z \sim 6$. The bulk of cosmic ionizations are produced by normal PopII stars in sufficiently massive galaxies (like the ones observed in UDF and GOODS). As these galaxies form, they create ionized (HII) regions around them, which continue to expand. The universe is half-ionized (by volume) at $z \sim 8 - 9$, and shortly before $z = 6$ most of cosmic HII regions merge during a relatively short period called “overlap”, completing the process of reionization of the universe.

Since it now appears that the Minimal Reionization Model provides the best theoretical framework for the existing data, it would make sense to refine its predictions and expectations to make a more precise comparison with the SDSS and

¹Particle Astrophysics Center, Fermi National Accelerator Laboratory, Batavia, IL 60510, USA; gnedin@fnal.gov

²Department of Astronomy & Astrophysics, The University of Chicago, Chicago, IL 60637 USA

³Steward Observatory, The University of Arizona, Tucson, AZ 85721; fan@as.arizona.edu

Table 1: Simulation Parameters

Run	L^a	Δx^b	ΔM^c	z_{OVL}^d	τ_{T}
L4N128	4	1	3.2×10^6	6.2	0.051
L8N128	8	2	2.6×10^7	6.2	0.048
L8N256	8	0.64	3.2×10^6	6.2	0.056

^aSize of the computational box in h^{-1} Mpc.

^bSpatial resolution in comoving h^{-1} kpc.

^cMass resolution in M_{\odot} .

^dBy construction.

WMAP data. It is particularly timely now, since several different groups make simulations of reionization, and these simulations rarely agree with each other.

In this paper we revisit the agreement with the data (or lack of it) for the simulations reported in Gnedin (2004), as well as for the latest simulation that is substantially larger and has much higher spatial resolution. The existence of a set of simulations with varied box sizes and mass and spatial resolutions allows us not only to compare the data to the model, but to also estimate the level of numerical convergence of the simulations, and, thus, make a rough estimate of the current theoretical uncertainty.

2. Simulations

In this paper we use three simulations that have different spatial and mass resolutions and different sizes of the simulation volumes, which allows us to estimate the degree of numerical convergence for different physical quantities. All simulations have been performed with the Softened Lagrangian Hydrodynamics (SLH) code (Gnedin 2000) using the Optically Thin Eddington Tensor (OTVET) approximation (Gnedin & Abel 2001) for following the time-dependent and spatial-variable transfer of ionizing radiation in 3D. All three simulations use the same cosmological parameters as reported in Spergel et al. (2003)¹

The numerical parameters of the simulations are listed in Table 1. The first two simulations are ones labeled “A4” and “A8” in Gnedin (2004) and Fan et al. (2006), while the third one is a new simulation with 256^3 dark matter particles,

¹ $\Omega_M = 0.27$, $\Omega_{\Lambda} = 0.73$, $h = 0.71$, $\Omega_B = 0.04$, $n_S = 1$.

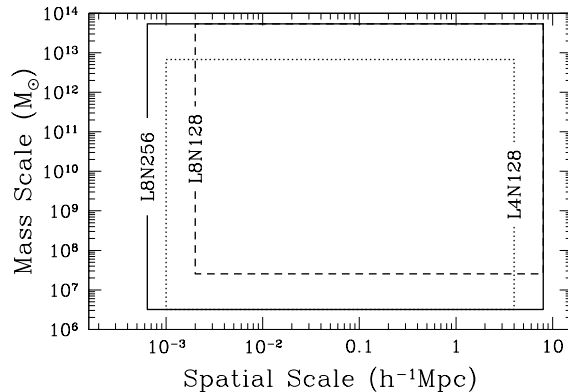


Fig. 1.— A graphical representation of the spatial and mass resolutions for the three simulations we use in this paper. The horizontal axis is the spatial scale and the vertical axis is the mass scale. Spatial and mass scales resolved in the three simulations are shown as three rectangles.

the same number of baryonic quasi-Lagrangian cells, and about 1,300,000 stellar particles that have been forming continuously during the simulation. In order to make references to specific simulations transparent, we label each simulation with a letter L followed by the value of the linear size of the computational volume (measured in h^{-1} Mpc in comoving reference frame), followed by the letter N and the number of dark matter particles (or baryonic cells) along one direction (128 or 256). For example, L4N128 means a simulation with $4h^{-1}$ Mpc box size and with 128^3 dark matter particles and an equal number of baryonic cells.

Table 1 also gives the nominal spatial resolution of the simulations (as measured by the value of Plummer softening length - the real resolution being a factor of 2-4 worse). Because of the specifics of the SLH method, a mesh with a larger number of cells can be deformed more, so the spatial resolution of the large L8N256 simulation is, in fact, higher than the spatial resolution of the L4N128 simulation, even if the mass resolutions of both simulations are identical.

Finally, we also list in Table 1 values for the redshift of overlap, z_{OVL} (Gnedin 2004), and the Thompson optical depth, τ_{T} , that we use below.

It is convenient to represent the numerical res-

olution of a given simulation as a rectangle in the spatial scale vs mass scale plane, as shown in Figure 1. The horizontal axis is the spatial scale (*not* a given spatial direction), and since a simulation has a finite spatial resolution and a finite box size, it is limited along the spatial axis at both ends. The same is true for the mass scale, so in the spatial scale - mass scale plane the simulation is represented by a rectangle. The three simulations are shown in Fig. 1. The L8N256 simulation has the largest spatial and mass dynamic range. The L8N128 run has the same box size as the L8N256, but lower spatial and mass resolution, while the L4N128 run has the same mass resolution as the L8N256 run, but lower box size (and somewhat lower spatial resolution, as explained above).

Because of the computational expense, and because our simulations become unreliable for $z < 5$ (as we explain below), the L8N256 run has been continued only until $z \sim 5$.

All simulations have been adjusted to best fit the mean transmitted flux data as explained in Gnedin (2004).

3. How to Simulate Reionization Correctly

Before we can compare the simulations and the data, it is important to explain why our simulations are adequate for modeling reionization, despite the limited box size. Modeling reionization, after all, is all about counting absorptions of ionizing photons correctly. It is well known that after reionization, absorption of ionizing photons is dominated by the Lyman Limit systems (Miralda-Escudé 2003). Obviously, the same should be true inside large enough HII regions even during reionization, so resolving the Lyman Limit systems is crucial for counting the absorptions of ionized photons correctly during and, perhaps, even before the overlap stage of reionization.

To illustrate this point, we show in Figure 2 a sketch of HII regions around two sources (a weak one and a strong one) before and after the overlap. Before overlap, most of photons emitted by a sufficiently weak source are absorbed by the neutral IGM just outside its I-front, while a sufficiently strong source, whose I-front reached the size comparable to the mean free path of ionizing photons inside it, effectively reaches its “Stromgen sphere”,

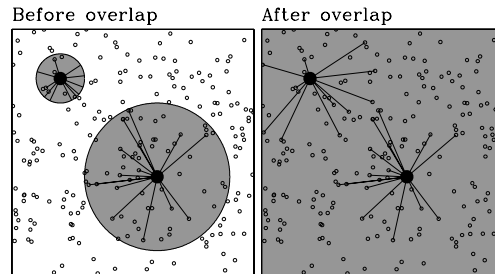


Fig. 2.— A sketch of two ionizing sources before and after overlap. Before overlap the mean free path for photons emitted by a weak source (in the upper left corner) is limited by the size of its HII region (gray area), while the strong source (in the lower right corner) has reached its Stromgen sphere and all photons it emits are absorbed in Lyman Limit systems (small open circles). After overlap, Lyman Limit system determine the mean free path for all sources.

because inside its HII region ionizations balance recombinations². After the overlap, all sources reach their “Stromgen spheres”, with ionization nearly balancing recombinations within the Lyman Limit systems (Miralda-Escudé et al. 2000).

The exact nature of Lyman Limit system is still rather poorly understood, but Lyman Limit systems in a simulation can still be studied by closely mimicking the observational process. The simulations we use in this paper do indeed resolve the Lyman Limit system (Kohler & Gnedin 2006) - in fact, they do it only too well by overpredicting the observed numbers of Lyman Limit systems at $z \sim 4$ by about a factor of 2 and by smaller factors at higher redshifts. The discrepancy is because the simulations do not properly include the ionizing radiation from quasars, and they become inadequate for describing the ionization state of the IGM for $z \lesssim 5$. This inadequacy at lower redshifts also becomes apparent in our results presented below.

Based on the analysis of the Lyman Limit systems from cosmological simulations we use here (Kohler & Gnedin 2006) it appears that spatial

²Note, that we use the term “Stromgen sphere” here differently from Shapiro & Giroux (1987), who did not account for Lyman Limit systems and thus concluded that cosmic HII regions never reach their Stromgen spheres.

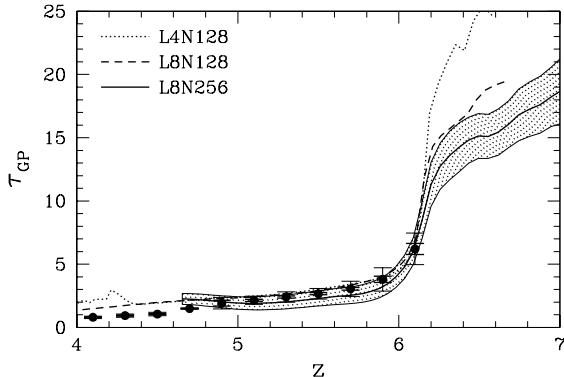


Fig. 3.— The mean Gunn-Peterson optical depth as a function of redshift for the simulations (gray lines) and data (black symbols). The dotted line shows the L4N128 run, the dashed line is for the L8N128 run, and the solid line is for our largest L8N256 run. In the latter case, the rms variation around the mean is shown as a hatched band. Filled circles show the observational data from Fan et al. (2006) with both rms dispersion (thin error-bars) and errors of the mean (thick error-bars).

resolution of at least 1-2 proper kpc is required to model the Lyman Limit systems correctly. Simulations of poorer spatial resolution would not be adequate for modeling cosmic reionization because they would underestimate absorption of ionizing radiation by a large factor.

4. Results

We first show in Figure 3 the evolution of the mean Gunn-Peterson optical depth, defined as

$$\tau_{\text{GP}} = -\log(\langle F(z) \rangle), \quad (1)$$

where $\langle F(z) \rangle$ is the mean (i.e. averaged over all possible directions) transmitted flux in the hydrogen Lyman- α transition at a given redshift. It is important to underscore that the mean Gunn-Peterson optical depth is *not* an average of anything, and, following Fan et al. (2006), we emphasize it by *not* using the overbar or the averaging operator $\langle \rangle$ in its definition.

The simulations are within about 10% of the data and within 10% of each other in the redshift interval $5 \lesssim z \lesssim 6.2$, but the agreement with the data for the $5.8 < z < 6.2$ interval is by construc-

tion - we adjust the effective emissivity parameter in the simulations to fit the observed data, as is explained in Gnedin (2004). The agreement in the interval $5 < z < 5.8$ is real - it reflects the fact that the ionization state of cosmic gas in the simulations is broadly consistent with the observational data (the following figures provide more detail on the level of agreement between the simulations and the data).

The fact that simulations with various box sizes and resolutions differ from each by about 10% demonstrates that our numerical results have not converged to that level of precision.

Formally, none of our three simulations is actually consistent with the data at $z < 5.8$ in the statistical sense - the simulations lie within the rms fluctuation in the Gunn-Peterson optical depth for a range of redshifts, but outside the formal errors in the mean value of τ_{GP} , which are about 5% for $z < 5.8$. However, the systematic errors in the measurement (continuum fitting and possible contaminations from BAL/metal absorption in Lyman- α forest region) are likely to be of the order of 5 to 10%, so the agreement between the simulations and the data at 10% level is satisfactory at present and is an encouraging confirmation of the Minimal Reionization Model.

We also emphasize the challenge facing the simulations in the years to come. As the random and especially systematic errors in the data are reduced, the current simulations will be hard pressed to fit the data at, say, 3 to 5% level. The future simulations will have to follow the radiative transfer correctly in fine detail to fit the observations, and this sensitivity to details offers a tremendous opportunity to learn about nature and distribution of ionizing sources at $z < 5.8$.

As we have mentioned above, the simulations become inadequate for $z < 5$ because they do not properly include the ionizing radiation from quasars. As the result, there are more Lyman Limit systems in the simulation (Kohler & Gnedin 2006), the IGM in the simulations is more neutral, and the mean free path of ionizing radiation for $z < 5$ is shorter than are actually observed.

At $z > 6.2$ the simulations show a marked lack of convergence in the mean Gunn-Peterson optical depth. This difference cannot be explained away entirely by cosmic variance, since the rms fluctua-

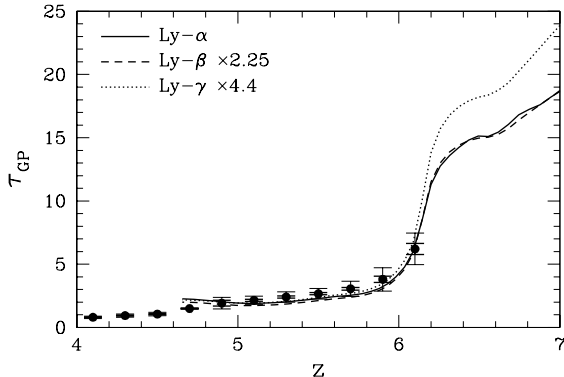


Fig. 4.— The mean Gunn-Peterson optical depth as a function of redshift for the L8N256 simulation (gray lines) and data (black symbols). The solid line shows the Lyman- α measurement (the same line as in Fig. 3), and dashed and dotted lines show the Lyman- β and Lyman- γ measurements respectively, rescaled to Lyman- α by factors 2.25 and 4.4, as used by Fan et al. (2006).

tions in, say, the L8N256 run are smaller than the difference between various runs.

This difference, however, is not surprising. After all, a mean Gunn-Peterson optical depth of 10 corresponds to the mean transmitted flux of only 10^{-5} - in a simulation with $128^3 \sim 2$ million cells only 20 transparent ($F = 1$) cells in the complete opaque ($F = 0$) medium would produce such a small mean transmitted flux. Thus, even discreteness effects in the simulation become important at these low values of the mean transmitted flux, in addition to usual effects of limited resolution, poorly known physics, lack of numerical convergence, etc - this is merely a statement of the fact that before the overlap any measurable transmission comes from the very tail of density and neutral fraction fluctuations, and, thus, is exceedingly difficult to simulate correctly. The latter statement only applies to the transmitted flux in the hydrogen Lyman- α transition, other quantities like mean fractions or photoionization rates can be modeled more reliably before the overlap.

It is also important to emphasize that the direct comparison between the simulations and the data for $\tau_{\text{GP}} > 10$ is highly non-trivial. The observational data constrain the Lyman- α optical depth directly only for $\tau_{\text{GP}} \lesssim 7$, and, for higher val-

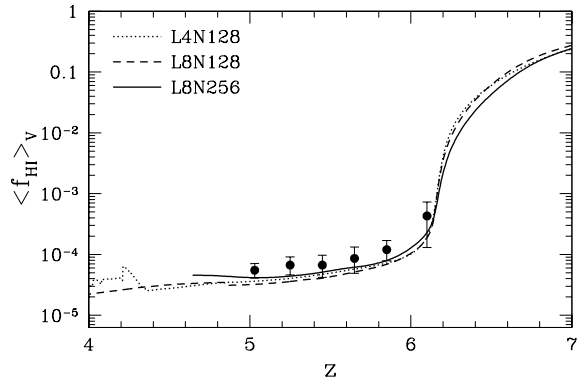


Fig. 5.— The mean volume-weighted neutral hydrogen fraction as a function of redshift for the simulations and data. The line and symbol markings are as in Fig. 3.

ues, properly rescaled constraints from Lyman- β and Lyman- γ transitions are used. When we repeat the Fan et al. (2006) rescaling procedure with our L8N256 simulation, we get a good agreement between the Lyman- β and Lyman- α for the scaling factor of 2.25, but get a higher optical depth for the Lyman- γ transition if we adopt Fan et al. (2006) scaling value of 4.4, while a smaller value of about 3.5 gives the best agreement between the Lyman- γ and Lyman- α measurements.

Figure 5 shows the comparison between the SDSS data and the simulations for the mean volume weighted neutral fraction³ as a function of redshift. In this quantity, the convergence of the simulations is much better, and the data are consistent (at 10 to 20% level) with the simulation results. This agreement is not surprising, given the agreement in the mean Gunn-Peterson optical depth - the neutral fraction (and the mean free path that we discuss below) is not measured directly from the observations, but is rather derived from the Gunn-Peterson optical depth measurement based on assumed density distribution of the IGM and photoionization equilibrium.

In Figure 6 we show the evolution of the mean

³The comparison is much more difficult for the mean mass weighted neutral fraction, because the simulations do not resolve Damped Lyman- α systems, that are known to contain most of neutral gas in the universe at $z \lesssim 4$, and are likely to contain at least a substantial fraction of all neutral gas at $z \lesssim 6$ as well.

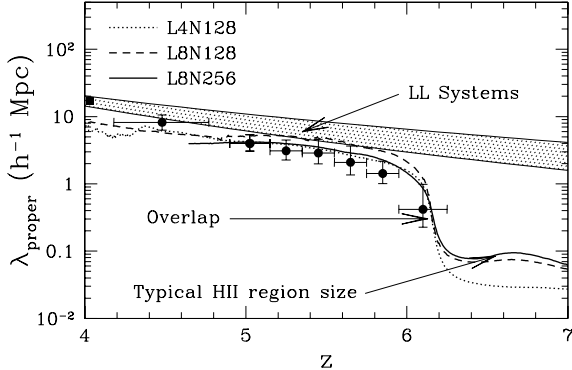


Fig. 6.— The mean free path of ionizing radiation as a function of redshift for the simulations and data. The line and symbol markings are as in Fig. 3. The filled black square at $z = 4$ shows the observational determination of the mean free path by Miralda-Escudé (2003), and the hatched black band is the extrapolation of the observed evolution of the Lyman Limit systems from Storrie-Lombardi et al. (1994) to $z > 4$.

free path of the Lyman Limit photons in the simulations and in the SDSS data, as well as a plausible extrapolation to high redshift of the mean free path from the Lyman Limit systems alone (Storrie-Lombardi et al. 1994; Miralda-Escudé 2003). As we have mentioned before, the simulations slightly underestimate the mean free path because they overpredict the abundance of the Lyman Limit systems up to a factor of 2 (Kohler & Gnedin 2006). The SDSS data only go up to the overlap epoch at $z \approx 6.2$, and are not yet able to probe the approach to the overlap at $z > 6.2$.

The SDSS estimate of the mean free path lies somewhat below the extrapolation from the Lyman Limit system measurement at $z = 4$. This difference is most likely not significant, as the extrapolation assumes a power-law evolution of Lyman Limit systems in redshift, which is too simple to be precise. But the general agreement between the extrapolation and the SDSS result indicates that the mean free path of Lyman Limit photons is limited by the Lyman Limit systems for $z < 5.8$, as is generally believed.

In the simulations, the strong deviation from the power-law evolution of the mean transmitted path with redshift at $z > 6$ indicates the over-

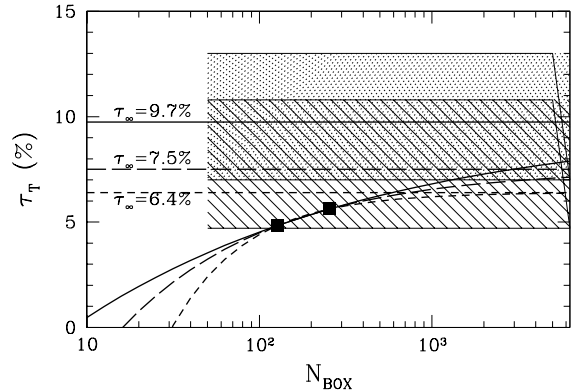


Fig. 7.— The Thompson optical depth as a function of resolution for the L8N128 and L8N256 simulations (black squares). The gray and black hatched bands show the constraints on τ_T from the *WMAP* polarization measurement alone ($\tau_T = 0.10 \pm 0.03$, Page (2006)) and from the combined *WMAP*+SDSS data ($\tau_T = 0.08 \pm 0.03$, Spergel (2006)) respectively. Black dotted, dashed, and solid curved lines show the fits to the simulation results in the form $\tau_T(N) = \tau_\infty + A/N^\alpha$ for $\alpha = 1, 1/2$, and $1/4$ respectively, while horizontal lines of the same type give the converged values τ_∞ .

lap stage of reionization - during which the mean free path is still determined by a typical size of HII regions rather than by the Lyman Limit systems. If we take the agreement between the SDSS data and the simulations for $z < 6.2$ as an indication that the rapid decrease in the SDSS estimate of the mean transmitted path indeed corresponds to the overlap of cosmic HII regions, then we can adopt the last SDSS data point as a plausible estimate of the time of overlap (formally defined as the moment when the mean free path grows most rapidly), giving $z_{\text{OVL}} = 6.1 \pm 0.15$.

In particular, the SDSS data limit the typical size of a cosmic HII region to less than about $1h^{-1}$ proper Mpc at $z \approx 6.2$.

Finally, we can compare the optical depth to Thompson scattering, τ_T , to the *WMAP* measurements. These values for the three simulations are given in Table 1 and also shown in Figure 7. As one can see, these values are far from being converged, because the smallest objects that form first (and are missed in finite resolution simulations) can contribute significantly to the Thompson op-

tical depth. In numerical analysis it is customary to estimate the converged result for any physical quantity C from a set of simulations with varied mesh size N by fitting the computed values of $C(N)$ with a functional form

$$C(N) = C_\infty + \frac{A}{N^\alpha}. \quad (2)$$

In order to determine three coefficients C_∞ , A , and α , three simulations with three different mesh sizes are required. Unfortunately, in our case it is not possible to get another simulation with a significantly different value of N : running a 512^3 SLH simulation is completely unfeasible now, and a 64^3 simulation is so small that it does not fit the SDSS data at all. Also, using a value of N somewhere between 128 and 256 would not help, as Fig. 7 illustrates.

In order to illustrate the inadequacy of our simulations for giving an accurate estimate of τ_T , we fitted equation (2) for the L8N128 and L8N256 simulations (since the resolution is the most important quantity for modeling the highest redshift star formation) keeping α as a free parameter, and fits for $\alpha = 1$, $1/2$, and $1/4$ are shown in Fig. 7. As anyone can see, the simulations are non-conclusive: depending on the rate of numerical convergence, the simulations can produce any value for τ_T between about 6 and 10%.

In addition, a significant (but not dominant) contribution from PopIII stars is also possible.

5. Conclusions

We have shown that numerical simulations of reionization that resolve the Lyman Limit systems (and, thus, correctly count absorptions of ionizing photons) are close (within 10% or so) to the SDSS data for a variety of measured and deduced quantities for $z < 6.2$. The SDSS data thus constraint the redshift of overlap to $z_{\text{OVL}} = 6.1 \pm 0.15$.

The mean free path of ionizing photons is limited by the Lyman Limit systems at $z < 6.0$, and is smaller at higher redshifts, reflecting a finite size of a typical cosmic HII region (less than $1h^{-1}$ proper Mpc at $z = 6.2$).

Our simulations, however, do not have nearly enough resolution to resolve the earliest episodes of star formation, and are very far from converging on the precise value of the optical depth to

Thompson scattering - any value between 6 and 10% is possible, depending on the convergence rate of the simulations and the fractional contribution of PopIII stars. This is generally consistent with the third-year *WMAP* results, but much higher resolution simulation are required to come up with the sufficiently precise value for the Thompson optical depth that can be statistically compared with the *WMAP* data.

While our simulations agree with the SDSS data within about 10% for $5 < z < 6.2$, the level of numerical convergence of simulations in this redshift interval is 10% at best. As the data improve (mostly by reducing the systematic errors), the constraining power of the SDSS data will be sufficient to place non-trivial demands on the degree of realism of any simulation that attempts to fit the data statistically. Not only the cosmological parameters in the simulation must be precise enough, but it is likely that fine details of radiative transfer (the relative roles of quasars and galaxies, their spatial clustering, accuracy of numerical schemes, etc) have to be done accurately as well. These requirements will present a challenge and a motivation for the future theoretical work on modeling cosmic reionization with greater precision than has been possible so far.

REFERENCES

- Fan, X., Strauss, M. A., Becker, R. H., White, R. L., Gunn, J. E., Knapp, G. R., Richards, G. T., Schneider, D. P., Brinkmann, J., & Fukugita, M. 2006, *AJ*, in press
- Gnedin, N. Y. 2000, *ApJ*, 535, 530
- . 2004, *ApJ*, 610, 9
- Gnedin, N. Y. & Abel, T. 2001, *New Astronomy*, 6, 437
- Kohler, K. & Gnedin, N. Y. 2006, *ApJ*, in preparation
- Melchiorri, A., Choudhury, T. R., Serra, P., & Ferrara, A. 2005, *MNRAS*, 364, 873
- Miralda-Escudé, J. 2003, *ApJ*, 597, 66
- Miralda-Escudé, J., Haehnelt, M., & Rees, M. J. 2000, *ApJ*, 530, 1
- Page, L. e. a. 2006, *ApJ*, submitted

Roy Choudhury, T. & Ferrara, A. 2006, astro-ph,
0603617

Shapiro, P. R. & Giroux, M. L. 1987, ApJ, 321,
L107

Spergel, D. N., Verde, L., Peiris, H., & et al. 2003,
ApJS, 148, 175

Spergel, D. N. e. a. 2006, ApJ, submitted

Storrie-Lombardi, L. J., McMahon, R. G., Irwin,
M. J., & Hazard, C. 1994, ApJ, 427, L13